The final publication is available at

http://doi.org/10.1039/c4nr00593g

Additional Information

Volume 1 | Number 1 | Jan 2013 | Pages 1–100

Nanoscale

www.rsc.org/nanoscale

ROYAL SOCIETY
OF CHEMISTRY
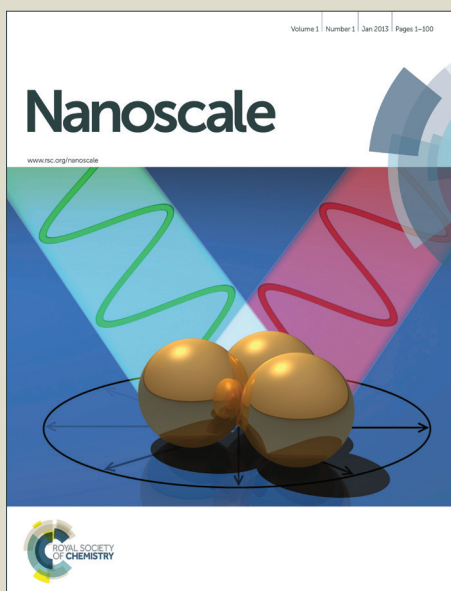
This is an *Accepted Manuscript*, which has been through the Royal Society of Chemistry peer review process and has been accepted for publication.

Accepted Manuscripts are published online shortly after acceptance, before technical editing, formatting and proof reading. Using this free service, authors can make their results available to the community, in citable form, before we publish the edited article. We will replace this *Accepted Manuscript* with the edited and formatted *Advance Article* as soon as it is available.

You can find more information about *Accepted Manuscripts* in the **Information for Authors**.

Please note that technical editing may introduce minor changes to the text and/or graphics, which may alter content. The journal's standard **Terms & Conditions** and the **Ethical guidelines** still apply. In no event shall the Royal Society of Chemistry be held responsible for any errors or omissions in this *Accepted Manuscript* or any consequences arising from the use of any information it contains.

Journal Name

COMMUNICATION

Silicon nanoparticles as Raman scattering enhancers

I. Rodriguez,[a] L. Shi,[a] X. Lu,[b] B. A. Korgel,[b] R. A. Alvarez-Puebla,[c,d,]* F. Meseguer,[a,]*

In this communication we demonstrate the large amplification values of the Raman signal of organic molecules attached to silicon nanoparticles (SiNPs). Light induced Mie resonances of high refractive index particles generate strong evanescent electromagnetic (EM) fields, thus boosting the Raman signal of species attached to the nanoparticles. The interest of this process is justified by the wide range of experimental configurations that can be implemented including photonic crystals, the sharp spectral resonances easily tuneable with the particle size, the biocompatibility and biodegradability of silicon, and the possibility of direct analysis of molecules that do not contain functional groups with high affinity for gold and silver. Additionally, silicon nanoparticles present stronger field enhancement due to Mie resonances at larger sizes than gold.

Metallic nanostructures and nanoparticles have attracted great attention in the last years as they have opened new fields of research as metamaterials.[1-3] The dramatic amplification of the Raman signal of organic species in close proximity to plasmonic nanoparticles, known as surface-enhanced Raman scattering[4,5] is widely used as a versatile analytical technique because of its multiplex capacity, possibility of remote sensing and ultrasensitive detection[6,7]. Nanoparticles of coinable metals show strong light scattering properties produced by the collective oscillations of their surface electrons (localized surface plasmon resonances, LSPR),[8,9] generating a huge evanescent electric field near the particle surfaces. As the Raman signal is proportional to the fourth power of the local electric field at the metal nanoparticle, the Raman amplification reaches values of up to 10^{10} in non-resonant molecules[10], giving rise to detection limits up to the single molecule level.[11,12] Although gold and silver are the most common plasmonic

metals, the concept of SERS has been extended to other nanomaterials like aluminum particles,[13] metal chalcogenides (including oxides, sulfides, selenides and tellurides)[14,15] or doped semiconductors with the capability of tuning the plasmon frequency through the dopant concentration[16]. Although SERS is considered a purely electromagnetic effect in nature, with contributions due to charge transfer, surface-assisted Raman amplification has been demonstrated with other materials such as quantum dots[17], or graphene.[18-20] In these cases, the SERS enhancement has been modest and can be attributed exclusively to chemical effects (i.e. resonant Raman effect induced by the optical transitions between electronic levels).

Large optical fields are, however, not exclusive of metallic particles. For example, large enhancement of the Raman cross-section has been predicted in Bloch surface waves of fully dielectric structures.[21,22] Further, high electrical fields can also be attained with micro and nanostructures.[23] In such materials, the strong scattering properties do not originate from collective excitations of electrons in the metal particle, but from the optical resonances of the whispering gallery modes (WGMs), also called Mie resonances, of nanostructures.[24,25] As a consequence of the large scattering cross section values, the Raman signal, of either any specie inside the cavities[26-29] or attached to them[30-33], is dramatically enhanced, this being termed silicon particle enhanced Raman scattering (SiPERS)[28]. Therefore, high refractive index nanostructures like silicon nanoparticles would also present huge fields not only inside the particles but also around them this allowing their use as SiPERS enhancers. However, although theory predicts very large Raman signal enhancement factors with similar values to those appearing for noble metals,[30] to the best of our knowledge, there are no experiments comparing the Raman

signal of chemical species attached to either, gold and high refractive index dielectric nanoparticles, like silicon. Silicon present several advantages over noble metals including low losses in the optical region, sharp wavelength Mie resonances strongly dependent on the particle size,[25,34] different surface chemistry, biocompatibility and biodegradability[35].

In this communication we proof the concept for the Raman amplification of minute concentrations of organic species attached to the surface of silicon nanoparticles. Implications of this demonstration include the expansion of the number of organic families that can be sampled directly with SERS usually restricted to those carrying functional groups with high affinity for gold and silver, the decrease in the price of production of this materials and the possibility of using single particles of larger sizes for optical monitoring with SERS.

Raman amplification is obtained on molecules in close proximity to the optical enhancer surfaces. The enhancement factor is related to the evanescent field around the particles, which, in turn, is also related to their scattering cross section values. The scattering cross section depends on the topology of the silicon nanoparticle. Figure 1 shows the scattering cross section of spherical silicon nanoparticles as a function of the size parameter value, k, defined as k=πd/λ, d and λ being the particle diameter and the light wavelength values respectively.

The spectra shown in the Figure 1 is a well-known universal profile, which does not depend on the particle size, provided the refractive index is not dispersive and the material has a
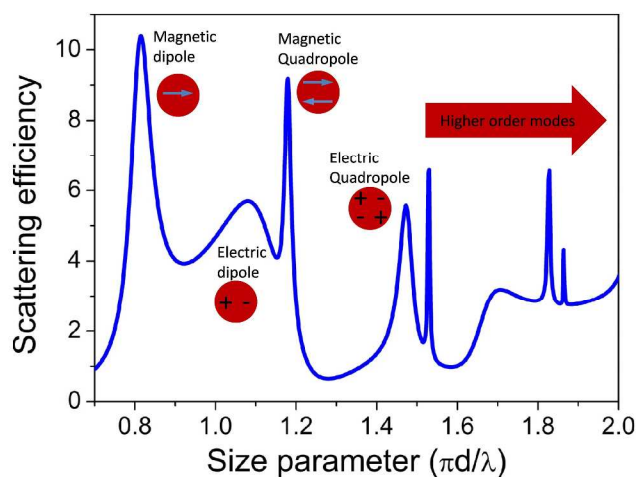

Fig. 1. Scattering efficiency of a single silicon spherical nanocavity as a function of the size parameter. We have assumed a constant value of the refractive index of Silicon (n=3.7).

small absorption value.[25] We have chosen a conventional NIR Raman laser wavelength (785 nm) for the proof of concept of our results, since this wavelength value is located in the transparency region of biological tissue (650-900 nm),[36] and because silicon shows a small absorption value. Notably, and in contrast to gold nanoparticles, the wavelength position of the Mie resonances of silicon can be

deeply tuned with the particle size.[25,34] Therefore, SiNPs may be suitable candidates for enhancing the Raman signal of the molecular species attached to them provided they are monodisperse. The calculation of the total evanescent field around the nanoparticles of different size when they are shined with the working laser line is shown in Figure 2. The input parameters are the particle size and the refractive index value of silicon in the wavelength region calculated (see the ESI). At difference to the gold case, SiNPs show narrow peaks at large particle size corresponding to high order Mie resonances and a broad structure at low values of the particle size coming from the low order modes resonances (see peaks adscription in Figure 1 and Figure 1S in the Electronic Supplementary Information, ESI). These results show that the evanescent field of the silicon nanoparticles is, roughly speaking, smaller than that of the gold ones. However, at certain particle size values where Mie modes resonate with the laser line, the evanescent field around silicon becomes of the same or even larger level intensity than those for gold plasmons. Gold nanoparticles also show peaks at certain
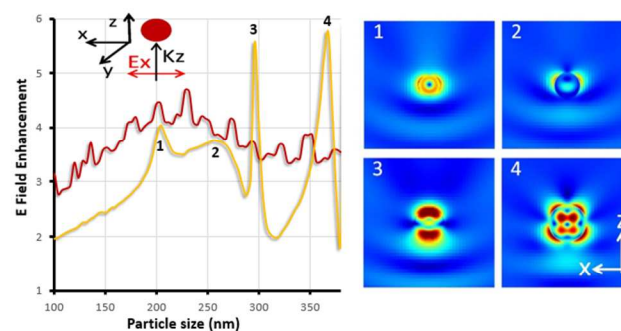

Fig. 2. Field enhancement around spherical particles of both silicon (yellow line) and gold (red line) as a function of the particle size when they are shined with a laser with a wavelength value of 785 nm, for particles embedded in air and the field distributions of the numbered peaks in the graph: (1) magnetic dipole, (2) electric dipole, (3) magnetic quadrupole, and (4) electric quadrupole modes.

particles values, but the strong damping effects of gold attenuate the resonances.

The processing of monodisperse spherical nanoparticles with a strict control of the particle size is a challenging goal that has been achieved in restricted cases for a limited range of sizes.[37,38] However, the limited size values reported,[37,38] do not allow tuning the lowest size parameter value Mie resonances. Also the refractive index of porous particles[37] is not high enough for boosting the Raman signal at intensity levels similar to those obtained from SERS on gold NPs. The spherical topology, a necessary condition, for sustaining Mie resonances as well as the monodisperse quality of SiNPs can be relaxed for low index modes appearing at low size parameters (see Figure 1). The broad resonances appearing in most of the Mie resonances of Figure 1 permit using non highly monodisperse silicon particles, provided the particles are non porous and they have the refractive index value of bulk silicon. Also, their EM field map plot would be less sensitive to the surface topology of the

nanocavities as the field map plots show in the Figure 2, and also in the ESI. Therefore as, at this stage, we cannot produce monodisperse spherical nanocavities with the appropriate particle diameter, we have processed monodisperse SiNPs with arbitrary surface topology with size values resonating at the four Mie resonances of the Figure 1 (see also Figure 1S in the ESI). The information
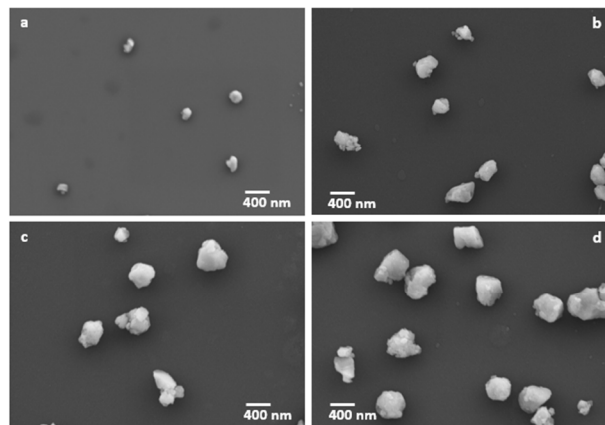

Fig. 3. SEM image of SiNPs obtained through mechanical milling of silicon powder together with a further particle separation through a colloidal sedimentation process: (a) 200, (b) 260, (c) 300 and (d) 370 nm.

~~reported below would give us information about the~~ potentiality of SiNPs as SiPERS enhancers even in the case they do not have a good spherical shape and good monodispersity values. We have processed silicon particles through mechanical milling of polycrystalline silicon. After several cycles of sedimentation,[39] we obtain monodisperse SiNPs with a refractive index value of bulk silicon (Figure 3).

The separation process allows for the selection of monodisperse SiNPs with particle size values where the evanescence field calculation shows maxima and with a reasonable monodispersity value of 10%. It important to stress that although the particles have not a spherical shape, both the high refractive index value, as well as the topology of resonances involved, allow them using as SiPERS enhancers, which will be reported next. In the following we will compare the Raman amplification signal from gold and silicon with the particle size values that maximizes their Raman signal.

To illustrate the Raman amplification efficiency and the surface composition of silicon and gold particles[40,41] on the SERS signal, samples were evaluated using p-aminobenzoic acid (PABA) as probe molecule.

Both gold and silicon nanoparticles were illuminated with near infrared laser (785 nm) as this laser line is conventional in many instruments. Also, it does not damage the sample as usually visible light does, and it is more appropriate for analysing biological samples as tissues are transparent to this radiation. As a first observation (Figure 4a), the SERS

intensity yielded by the gold nanoparticles show maximum values for particle size values around 100 nm. For increasing particle size, the SERS signal decreases due to the increasing contribution of the radioactive damping which is, consistent with previous reports[40]. In the case of SiNPs, SiPERS signals of PABA were identified from sizes around 200, 260, 300 and 370 nm, which roughly correspond to the calculated particle size values where the laser line resonate (see peaks 1-4 in figure 2). It is worthy to note that for both cases spectral shapes remains stable from particle to particle while intensity slightly fluctuates (see Figure 4a) as commonly observed in this kind of experiments with a Raman amplifications factor of 10^6, a usual value for isolated particles.

Calculation of the scattering cross-sections of silicon spherical particles as a function of the illumination wavelength (Figures 1 and 1S in the ESI) shows that these colloids exhibit several resonances at the low modal number Mie resonances, specifically magnetic dipole (Figure 1Sa), electric dipole (Figure 1Sb), magnetic quadrupole (Figure 1Sc) and electric quadrupole mode (Figure 1Sd) for sizes of 204, 256, 296 and 368 nm, respectively. Differences in the intensity are ascribed, first to the increase of the near electric field generated by each mode, but also to the lower sphericity of the particles produced by mechanical milling. Notably, although in plasmonic particles the Raman amplification mainly relies on the electric fields generated by the electric dipolar plasmon resonances, in the case of silicon, fields are related to the higher order electric and magnetic Mie modes.[23,25]

SERS and SiPERS spectra of PABA also illustrate the effect of the surface chemistry of the particle on the Raman signal. PABA contains two different functionalities in the opposite parts of its aromatic ring, an amino, and a carboxylic acid groups. These groups show different affinity for each surface. While the amino group presents strong interactions with gold surfaces, carboxylic groups prefer silicon surfaces. SERS spectra of PABA as a function of optical enhancer are shown in the Figure 4b. The SERS spectrum on gold is similar to those previously reported for PABA[42], where the molecule is adsorbed through the amino group. The vibrational frequencies observed on the gold-PABA spectrum fit band to band with the Raman spectrum of the PABA in bulk. However, the relative intensities in the SERS spectrum show strong enhancement of the v19a ring mode (1515 cm^{-1}) and the band corresponding to the rocking vibration of the amino group (983 cm^{-1}) [43]. In fact, the increase in relative intensity of this band can be explained if the amino group is directly attached to the gold surface. Additionally, the band at 1700 cm^{-1} assigned to the C=O stretching is not visible in the Raman spectrum. The reason of the appearance of this band may be explained because of the complex formed between the amino group and gold. Gold colloids are strong electron-donors, thus, when the PABA is attached to them, the aromatic rings become electron acceptors, hindering the dissociation of the

carboxylic group. The presence of ν(C=O) band strongly supports the hypothesis that the carboxylic group is not interacting with the surface. Notably, when SiPERS is carried out on the silicon colloids, the spectrum shows changes in the relative intensity of the bands. First, the band
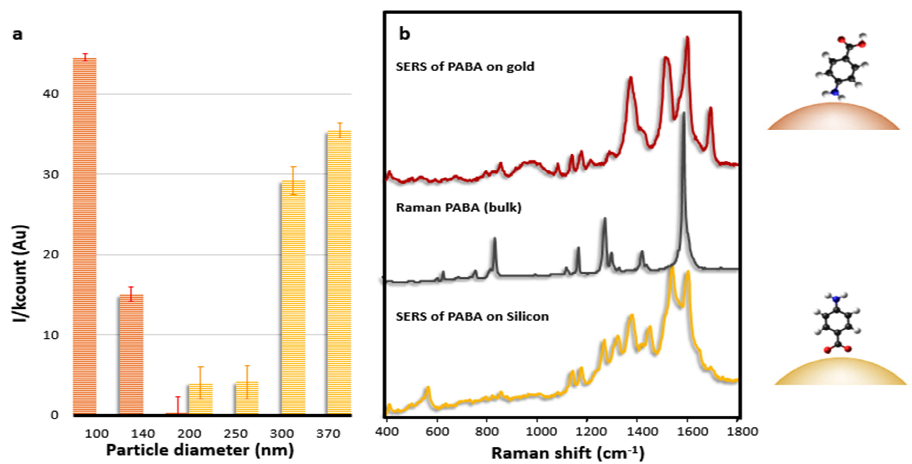
Fig. 4. (a) Intensities and (b) SERS spectra of PABA excited at 785 nm on colloidal dispersions of gold (100-400 nm) and silicon (200-370 nm) particles. Gold (red) and silicon (yellow).

at 1515 cm^{-1} (ν19a) decreases while those at 1450 cm^{-1} (ν19b) increases indicating a change in the molecular orientation with respect to the surface. Further, and more important, the C=O stretching mode (1700 cm^{-1} band) disappears suggesting a direct interaction between the silicon surfaces and the carboxylic group. This hypothesis is also supported because of the emergence of a strong new band at 1542 cm^{-1} that could be assigned to the NH$_2$ asymmetric deformation.

Conclusions

To conclude herein we show the great potentiality of SiNPs as Raman signal enhancers of organic molecules attached to them and, induced by the huge evanescent fields associated to the Mie resonances of non-spherical shape nanoparticles. It may open the door for the generation of a new biocompatible, and biodegradable[35,44] surface for biosensing, easily attainable with standard particles processing techniques. Further, these new active optical surfaces show different affinities to the conventional plasmonic noble metals paving the road for the direct analysis of families of molecules difficult to detect with gold or silver due to their small affinity with such metals.

Notes and references

[a] Centro de Tecnologías Físicas, Unidad Asociada ICMM/CSIC-UPV, Universidad Politécnica de Valencia, Av. Los Naranjos s/n, Valencia, 46022 Spain and Instituto de Ciencia de Materiales de Madrid, CSIC, Madrid, 28049 Spain. Email: fmese@fis.upv.es.

[b] Department of Chemical Engineering, Texas Materials Institute and Center for Nano- and Molecular Science and Technology, The University of Texas at Austin, Austin, Texas 78712-1062, United States.

[c] Departamento de Quimica Fisica e Inorganica, Universitat Rovira i Virgili and Centro de Tecnología Química de Catalunya, Carrer de Marcel•lí Domingo s/n, 43007 Tarragona, Spain. Email: ramon.alvarez@urv.cat.

[d] ICREA, Passeig Lluís Companys 23, 08010 Barcelona, Spain.

1 C. M. Soukoulis, and M. Wegener, *Nature Photonics*, 2011, **5**, 523.

2 W. Cai, and V. Shalaev, *Optical Metamaterials: Fundamentals and Applications*. Springer, 2010.

3 R. Merlin, Science, 2007, **317**, 927.

4 P. L. Stiles, J. A. Dieringer, N. C. Shah, and R. P. Van Duyne, *An. Rev. Anal. Chem.*, 2008, **1**, 601.

5 M. Moskovits, *Notes Rec. Royal Soc.*, 2012, **66**, 195.

6 R. A. Alvarez-Puebla, and L. M. Liz-Marzán, Angew. *Chem. Int. Ed.*, 2012, **51**, 11214.

7 R. S. Golightly, W. E. Doering, M. J. Natan, *ACS Nano*, 2009, **3**, 2859.

8 U. Kreibig, and M.Vollmer, *Optical properties of metal clusters*, Springer, 1995.

9 N. J. Halas, S. Lal, W-S. Chang, S. Link, P. Nordlander, *Chem. Rev.*, 2011, **111**, 3913.

10 L. Rodriguez-Lorenzo, R. A. Alvarez-Puebla, I. Pastoriza-Santos, S. Mazzucco, O. Stephan, M. Kociak, L. M. Liz-Marzan, F. J. Garcia de Abajo, *J. Am. Chem. Soc.*, 2009, **131**, 4616.

11 E. Cortés, P. G. Etchegoin, E. C. Le Ru, A. Fainstein, M. E. Vela, R. C. Salvarezza, *J. Am. Chem. Soc.*, 2013, **135**, 2809.

12 N. P. W. Pieczonka, R. F. Aroca, *Chem. Soc. Rev.*, 2008, **37**, 946.

13 M. W. Knight, L. Liu, Y. Wang, L. Brown, S. Mukherjee, N. S. King, H. O. Everitt, P. Nordlander, N. J. Halas, *Nano Lett.*, 2012, **12**, 6000.

14 L. Li,. T. Hutter,; A. S. Finnemore, F. M. Huang, J. J. Baumberg, S. R. Elliott, U. Steiner, S. Mahajan, *Nano Lett.*, 2012, **12,** 4242.

15 W. Li, R. Zamani, P. Rivera-Gil, B. Pelaz, M. Ibáñez, D. Cadavid, A. Shavel, R. A. Alvarez-Puebla, W. J. Parak, J. Arbiol, A. Cabot, *J. Am. Chem. Soc.*, 2013, **135**, 7098.

16 D. J. Rowe, J. S. Jeong, K. A. Mkhoyan, U. R. Kortshagen, *Nano Lett.*, 2013, **13**, 1317.

17 Y. Wang, J. Zhang, H. Jia, M. Li, J. Zeng, B. Yang, B. Zhao, W. Xu, J. R. Lombardi, *J. Phys. Chem. C*, 2008, **112**, 996.

18 M. Begliarbekov, O. Sul, J. Santanello, N. Ai, X. Zhang, E. H. Yang, S. Strauf, *Nano Lett.*, 2011, **11**, 1254.

19 X. Ling, L. Xie, Y. Fang, H. Xu, H. Zhang, J. Kong, M. S. Dresselhaus, J. Zhang, Z. Liu, *Nano Lett.*, 2009, **10**, 553.

20 E. S. Thrall, A. C. Crowther, Z. Yu, L. E. Brus, *Nano Lett.*, 2012, **12**, 1571.

21 A. Delfan, M. Liscidini, J. E. Sipe, *J. Opt. Soc. Am. B*, 2012, **29**, 1863.

22 S. Pirotta, X. G. Xu, A. Delfan, S. Mysore, S. Maiti, G. Dacarro, M. Patrini, M. Galli, G. Guizzetti, D. Bajoni, J. E. Sipe, G. C. Walker, M. Liscidini, *J. Phys. Chem. C,* 2013, **117,** 6821.

23 C. F. Bohren, D. R. Huffman, *Absorption and scattering of light by small particles,* Wiley, 1983.

24 J. D. Eversole, H.-B. Lin, A. L. Huston, and A. J. Campillo, *J. Opt. Soc. Am. A,* 1990, **7**, 2159.

25 L. Shi, T. U. Tuzer, R. Fenollosa, F. Meseguer, *Adv. Mater.*, 2012, **24**, 5934.

26 D. V. Murphy, and S.R. J. Brueck, *Optics Letters*, 1983, **8**, 494.

27 J. B. Snow, S.-X. Qian, and R. K. Chang, *Opt. Lett.* 1985, **10**, 37.

28 R. Symes, R. M. Sayer, and J. P. Reid, *Phys. Chem. Chem. Phys.* 2004, **6**, 474.

29 R. J. Hopkins and J. P. Reid, *J. Phys. Chem.* B, 2006, **110**, 3239.

30 L. K.Ausman, G. C. Schatz, *J. Chem. Phys,.* 2008, **129**, 054704.

31 M. S. Andersson, *Appl. Phys. Lett.*, 2010, **97**, 131116.

32 I. Alessandri, *J. Am. Chem. Soc*, 2013, **135**, 5541.

33 S. M. Wells, I. A. Merkulov, I. I. Kravchenko, N. V. Lavrik, and M. J. Sepaniak, *ACS Nano,* 2012, **6**, 2948.

34 E. Xifré-Pérez, R. Fenollosa, and F. Meseguer, *Optics Express*, 2011, **19**, 3455.

35 L. T. Canham, *Adv. Mater.*, 1995, **7**, 1033.

36 R. Weissleder, *Nat. Biotechnol.,* 2001, **19**, 321.

37 L. Shi, J. T. Harris, R.Fenollosa, I. Rodriguez, X. Lu, B. A. Korgel, F. Meseguer, *Nat. Comm.,* 2013, **4**, 1904.

38 A. Gumennik, L Wei, G. Lestoquoy, A. M. Stolyarov, X. Jia, P. H. Rekemeyer, M. J. Smith, X. Lianf, B. J.-B. Grena, S. G. Johnson, S. Gradecak, A. F. Abouraddy J. D. Joannopoulos, and Y. Fink et al., *Nat. Comm.*, 2013, **4**, 2216.

39 I. Rodriguez, R. Fenollosa, F. Meseguer, and A. Perez-Roldan, 2011, ES 2386126; WO 2012101306.

40 N. Pazos-Perez, F. J. Garcia de Abajo, A. Fery, and R. A. Alvarez-Puebla, *Langmuir*, 2012, **28**, 8909.

41 N. G. Bastús, J. Comenge, V. Puntes, *Langmuir*, 2011, **27**, 11098.

42 S. Sánchez-Cortés, J. V. Garcia-Ramos, G. Morcillo, *J. Colloid Interface Sci.*, 1994, **167**, 428.

43 H. Park, S. B. Lee, K. Kim, M. S. J. Kim, Phys. Chem., 1990, **94**, 7576.

44 J.H. Park, L. Gu, G. von Maltzahn, E. Ruoslahti, S. N. Bhatia, M. J. Sailor, *Nat. Mater.,* 2009, **8**, 331.